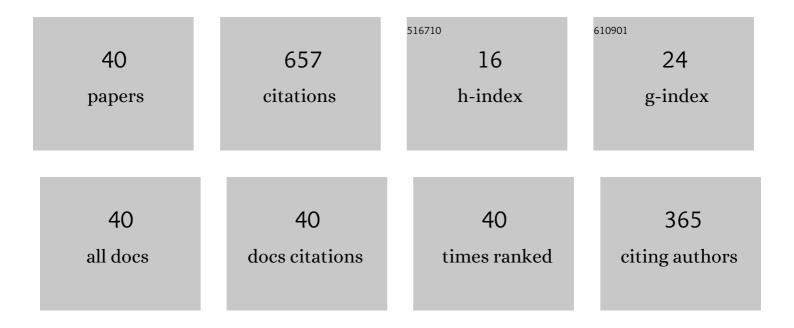
Laiqi Zhang

List of Publications by Year in descending order

Source: https://exaly.com/author-pdf/1014767/publications.pdf Version: 2024-02-01



Ι ΔΙΟΙ ΖΗΔΝΟ

#	Article	IF	CITATIONS
1	Reaction behavior and pore formation mechanism of TiAl–Nb porous alloys prepared by elemental powder metallurgy. Intermetallics, 2014, 44, 1-7.	3.9	47
2	Microstructure and properties of Al alloy ER5183 deposited by variable polarity cold metal transfer. Journal of Materials Processing Technology, 2019, 267, 167-176.	6.3	45
3	Oxidation behavior of Mo-Si-B alloys at medium-to-high temperatures. Journal of Materials Science and Technology, 2021, 60, 113-127.	10.7	45
4	Pore structure and gas permeability of high Nb-containing TiAl porous alloys by elemental powder metallurgy for microfiltration application. Intermetallics, 2013, 33, 2-7.	3.9	42
5	Fe-Al intermetallic foam with porosity above 60 % prepared by thermal explosion. Journal of Alloys and Compounds, 2018, 732, 443-447.	5.5	39
6	Characterization of microstructure evolution in $\hat{I}^2 \cdot \hat{I}^3$ TiAl alloy containing high content of Niobium using constitutive equation and power dissipation map. Materials and Design, 2016, 107, 406-415.	7.0	36
7	Effect of martensite morphology and volume fraction on the low-temperature impact toughness of dual-phase steels. Materials Science & Engineering A: Structural Materials: Properties, Microstructure and Processing, 2022, 832, 142424.	5.6	35
8	Complete elimination of pest oxidation by high entropy refractory metallic silicide (Mo0.2W0.2Cr0.2Ta0.2Nb0.2)Si2. Scripta Materialia, 2020, 189, 25-29.	5.2	31
9	Preparation, microstructure, and constitutive equation of W-0.25 wt% Al2O3 alloy. Materials Science & Engineering A: Structural Materials: Properties, Microstructure and Processing, 2019, 744, 79-85.	5.6	29
10	Fracture toughness and fracture mechanisms in Mo5SiB2 at ambient to elevated temperatures. Intermetallics, 2013, 38, 49-54.	3.9	28
11	Constitutive modeling of high temperature flow behavior in a Ti-45Al-8Nb-2Cr-2Mn-0.2Y alloy. Scientific Reports, 2018, 8, 5453.	3.3	28
12	Hierarchical porous TiAl3 intermetallics synthesized by thermal explosion with a leachable space-holder material. Materials Letters, 2016, 181, 261-264.	2.6	26
13	Spark plasma sintering synthesis of intermetallic T2 in the Mo–Si–B system. Advanced Powder Technology, 2013, 24, 913-920.	4.1	22
14	A novel of MSi2 high-entropy silicide: Be expected to improve mechanical properties of MoSi2. Materials Letters, 2020, 268, 127629.	2.6	22
15	Intrinsic embrittlement of MoSi2 and alloying effect on ductility: Studied by first-principles. Physica B: Condensed Matter, 2010, 405, 1695-1700.	2.7	19
16	Effect of ZrO2 content on microstructure and mechanical properties of W alloys fabricated by spark plasma sintering. International Journal of Refractory Metals and Hard Materials, 2019, 79, 79-89.	3.8	17
17	Microstructural instability in surface layer of a high Nb-TiAl alloy processed by shot peening following high temperature exposure. Intermetallics, 2016, 78, 8-16.	3.9	14
18	Deformation behavior of Mo5SiB2 at elevated temperatures. Materials Science & Engineering A: Structural Materials: Properties, Microstructure and Processing, 2015, 623, 124-132.	5.6	12

Laiqi Zhang

#	Article	IF	CITATIONS
19	Intrinsic brittleness of Mo5SiB2 and alloying effect on ductility studied by first-principles calculations. Intermetallics, 2014, 50, 79-85.	3.9	10
20	Joining of β-γ TiAl alloys containing high content of niobium by pulse current diffusion bonding. Intermetallics, 2021, 133, 107184.	3.9	10
21	Kinetic and thermodynamic properties of liquid zinc: An ab initio molecular dynamics study. Computational Materials Science, 2018, 141, 180-184.	3.0	9
22	Pore/skeleton structure and compressive strength of porous Mo3Si-Mo5Si3-Mo5SiB2 intermetallic compounds prepared by spark plasma sintering and homogenization treatment. Journal of Alloys and Compounds, 2021, 856, 158150.	5.5	9
23	Ab initio investigation of phase stability, thermo-physical and mechanical properties of (Mo0.2Cr0.2Ta0.2Nb0.2X0.2)Si2 (XÂ=ÂW, V) high-entropy refractory metal silicides. Computational Materials Science, 2022, 203, 111116.	3.0	8
24	Improvement in the liquid zinc corrosion resistance of high Nb-TiAl alloys by pre-oxidation in a SiO2-powder pack. Science China Technological Sciences, 2012, 55, 505-509.	4.0	7
25	Characteristics and Thermal Shock Resistance of HVOF-Sprayed TiAlNb Coatings. Journal of Thermal Spray Technology, 2020, 29, 1752-1762.	3.1	7
26	Effect of Al2O3 content and swaging on microstructure and mechanical properties of Al2O3/W alloys. International Journal of Refractory Metals and Hard Materials, 2020, 86, 105082.	3.8	6
27	A study of residual Ti3Al in γ(TiAl) sheets using mismatch theory. Materials Letters, 2020, 278, 128423.	2.6	6
28	Dislocation climb in Mo 5 SiB 2 during high-temperature deformation. International Journal of Refractory Metals and Hard Materials, 2016, 61, 115-120.	3.8	5
29	A method by calculation of wetting angle for designing of the corrosion-resistant materials in hot-dip galvanizing. Solid State Communications, 2021, 323, 114102.	1.9	5
30	Hot deformation behavior and artificial neural network modeling of β-γ TiAl alloy containing high content of Nb. Materials Today Communications, 2021, 27, 102405.	1.9	5
31	Achievement of forging without canning for β-solidifying γ-TiAl alloy containing high content of niobium. Materials and Manufacturing Processes, 2021, 36, 1667-1676.	4.7	5
32	Oxygen removal from raw silicon powder by the HFâ€ethanol solution etching. Surface and Interface Analysis, 2013, 45, 955-961.	1.8	4
33	Fabrication of a multi-phase porous high-temperature Mo–Si–B alloy by <i>in situ</i> reaction synthesis. Powder Metallurgy, 2019, 62, 258-266.	1.7	4
34	Molecular Dynamics Simulation of the Tensile Deformation Behavior of the γ(TiAl)/α2(Ti3Al) Interface at Different Temperatures. Journal of Materials Engineering and Performance, 2022, 31, 918-932.	2.5	4
35	Effect of transition metal alloying elements on the deformation of Ti-44Al-8Nb-0.2B-0.2Y alloys. Scientific Reports, 2018, 8, 14242.	3.3	3
36	Competitive mechanism of phosphorus capturing between MC-carbide (MÂ=ÂTi, Mo) and ferrite/martensite interface in dual-phase steel. Materials Letters, 2021, 283, 128820.	2.6	3

Laiqi Zhang

#	Article	IF	CITATIONS
37	Corrosion resistance of TiAl–Nb coating on 316L stainless steel in liquid zinc. Journal of Materials Science, 2021, 56, 4022-4033.	3.7	3
38	Characterization of the Trace Phosphorus Segregation and Mechanical Properties of Dual-Phase Steels. Acta Metallurgica Sinica (English Letters), 0, , 1.	2.9	3
39	Interfacial microstructure and shear performance of TiAl to Nb–Si alloy diffusion bonded with pure Ti interlayer. Intermetallics, 2022, 146, 107569.	3.9	3
40	Double-pore structure porous Mo–Si–B intermetallics fabricated by elemental powder metallurgy method using NH4HCO3 as pore-forming agent. Materials Research Express, 2020, 7, 096518.	1.6	1